

RESEARCH

Open Access



# Single cell RNA-seq analysis reveals temporally-regulated and quiescence-regulated gene expression in *Drosophila* larval neuroblasts

Noah Dillon<sup>1</sup> , Ben Cocanougher<sup>2</sup>, Chhavi Sood<sup>3</sup>, Xin Yuan<sup>3</sup>, Andrea B Kohn<sup>4</sup>, Leonid L Moroz<sup>4</sup>, Sarah E Siegrist<sup>3</sup> , Marta Zlatic<sup>5,6</sup> and Chris Q. Doe<sup>1\*</sup>

## Abstract

The mechanisms that generate neural diversity during development remains largely unknown. Here, we use scRNA-seq methodology to discover new features of the *Drosophila* larval CNS across several key developmental timepoints. We identify multiple progenitor subtypes – both stem cell-like neuroblasts and intermediate progenitors – that change gene expression across larval development, and report on new candidate markers for each class of progenitors. We identify a pool of quiescent neuroblasts in newly hatched larvae and show that they are transcriptionally primed to respond to the insulin signaling pathway to exit from quiescence, including relevant pathway components in the adjacent glial signaling cell type. We identify candidate “temporal transcription factors” (TTFs) that are expressed at different times in progenitor lineages. Our work identifies many cell type specific genes that are candidates for functional roles, and generates new insight into the differentiation trajectory of larval neurons.

**Keywords:** Neuroblast, Intermediate neural progenitor, Temporal transcription factor, Single cell RNA-sequencing, Quiescence, Insulin signaling

## Introduction

A major question in neuroscience is how neural diversity is generated, which underlies complex neural circuits and behavioral output of the central nervous system (CNS). In the past, neuronal diversity was commonly defined by morphological features (axon/dendrite processes), biochemical features (neurotransmitter choice), and physiological features (distinct ion channels and membrane properties) [1]. In addition, “low throughput” assays for molecular differences among neurons, typically for transcription factor (TF) expression, have been crucial for

finding insights into the generation of neural diversity for decades [2, 3]. Taken together, these approaches resulted in the definition various classes or subtypes of motor neurons, interneurons, sensory neurons and peptidergic neurons, but they are ill-suited to address the question of how many unique types of neurons exist within the CNS, and the subsequent question of how each cell type contributes to the function of the CNS.

The advent of single cell RNA sequencing (scRNA-seq) allowed a more complete inventory of gene expression profiles within individual neurons, with the expression of “validated cell type genes” used as a framework to identify transcriptionally related neurons [4–8]. Further analysis has revealed novel cell types based on common gene expression, but also that trajectories between cell types to be more gradual and less saltatory than previously

\*Correspondence: [cdoe@uoregon.edu](mailto:cdoe@uoregon.edu)

<sup>1</sup> Institute of Neuroscience, Howard Hughes Medical Institute, University of Oregon, OR 97403 Eugene, USA  
Full list of author information is available at the end of the article



© The Author(s) 2022. **Open Access** This article is licensed under a Creative Commons Attribution 4.0 International License, which permits use, sharing, adaptation, distribution and reproduction in any medium or format, as long as you give appropriate credit to the original author(s) and the source, provide a link to the Creative Commons licence, and indicate if changes were made. The images or other third party material in this article are included in the article's Creative Commons licence, unless indicated otherwise in a credit line to the material. If material is not included in the article's Creative Commons licence and your intended use is not permitted by statutory regulation or exceeds the permitted use, you will need to obtain permission directly from the copyright holder. To view a copy of this licence, visit <http://creativecommons.org/licenses/by/4.0/>. The Creative Commons Public Domain Dedication waiver (<http://creativecommons.org/publicdomain/zero/1.0/>) applies to the data made available in this article, unless otherwise stated in a credit line to the data.

appreciated, in part due to transcriptional priming [9–11].

In *Drosophila*, neuronal scRNA-seq has been done on adult brain [12–16], pupae [17–22], larvae [23–25], and blastoderm-stage embryos [26]. These experiments have provided valuable insight into the number of distinct neuronal types and identified gene candidates for regulating neural subtype function or connectivity. However, no studies to date have focused on identifying and characterizing the transcriptional diversity of neural progenitors, nor has any study mapped progenitor transcriptional profile at multiple larval stages. In this study, we identify multiple progenitor subtypes across several larval stages with differential gene expression to provide candidate genes as cell type specific markers and functional roles during development.

## Results

### Larval atlas shows distinct cell identities and differentiating neural progenitor axis

To identify single cell gene expression profiles throughout larval development, we used scRNA-seq data collected by [27] from dissociated brain and ventral nerve cord (VNC) – together termed the CNS – from larvae at 1h, 24h and 48h (all times in hours after larval hatching; ALH). We used the 10X Genomics pipeline for scRNA-seq analysis and used Cell Ranger Aggregation to aggregate multiple samples from the same timepoint. We used the standard Seurat integration pipeline to filter out low quality cells and clustered 97,845 cells from all larval stages (see methods; Fig. 1a). Within our atlas we identified clusters enriched for cell types in the CNS: neural progenitors, immature and mature neurons, glia, trachea, hemocytes and insulin-producing cells (IPCs; Fig. 1a; Supp. Table 1). Representative examples of a progenitor marker (Deadpan; *dpn*), a new-born neuron marker (*Hey*), a maturing neuron marker (*nSyb*), and a glia marker (*repo*) are shown in Fig. 1b.

We next focused on the progenitor and immature neuron cluster, sub-clustering only these cells. We found clear separation of the major progenitor cell types: quiescent neuroblasts (cluster 12), type I neuroblasts (cluster 9), type II neuroblasts (cluster 2), Intermediate Neural Progenitors (INPs, cluster 3), Ganglion Mother Cells (GMCs, cluster 1), new-born neurons (cluster 8), and immature neurons (clusters 0, 4–6, 10, and 11), plus one low quality cluster (7) that was excluded from subsequent analysis (Fig. 1c; Supp. Table 2). Clusters were assigned cell type designations based on enriched expression of experimentally validated cell type markers (Fig. 1c; Table 1). Interestingly, each class of progenitor formed a distinct cluster, creating a differentiation axis right to left in UMAP space (Fig. 1d). Not surprisingly, the quiescent

neuroblast cluster was enriched at 1h when most neuroblasts are quiescent [28], followed by emergence of proliferating neuroblasts, INP and GMC clusters at 24h and 48h (Fig. 1e). Thus, we can identify and transcriptionally profile all known progenitor subtypes across larval development, including quiescent neuroblasts which have never been identified in RNA-seq experiments. We discuss each progenitor type in more detail below (Tables 2 and 3).

### Quiescent neuroblasts and associated glia are enriched for expression of genes regulating the TOR and insulin pathways

The majority of neuroblasts enter quiescence before the end of embryogenesis and remain quiescent until 12–24h [71, 72]. We noticed that cluster 12 is clearly present at 1h but the number of cells drop at 24h and 48h (Fig. 2a–b); this timing coincides with neuroblasts exiting quiescence. We confirmed this cluster 12 identity as quiescent neuroblasts using the positive markers *dpn* and *trbls* in addition to the lack of expression of canonical proliferating neuroblast markers (Fig. 2c; Table 1; Supp. Table 2). The top cluster defining genes (i.e., genes that define the cluster as a distinct grouping of cells) represented cell growth, cell cycle progression and the insulin signaling pathway (Fig. 2c).

To further investigate gene expression in this quiescent neuroblast population, we analyzed the expression of core elements regulating the insulin receptor (*InR*), AKT pathway, TOR pathway and general markers of cell growth. We were interested in *InR* regulation in quiescent neuroblasts because previous work has showed insulin signaling to be essential for neuroblasts to exit quiescence [28, 74]. We found upregulation of *InR* in addition to upregulation of positive regulators for *InR* (Fig. 2d). AKT and TOR genes showed lower expression (Fig. 2d), consistent with the lack of cellular growth in quiescent neuroblasts. Similarly, markers for cell cycle genes showed low expression (Fig. 2d). We conclude that quiescent neuroblasts are transcriptionally primed to receive insulin signaling but have yet to initiate proliferation and growth.

Previous work has found that insulin signaling from glia is required for neuroblasts to exit quiescence [28]. To investigate this connection, we explored glial gene expression related to neuroblast quiescent signaling pathways. We sub-clustered from the whole atlas 11,004 cells from clusters that were positive for the pan glial marker *repo* (Fig. 2e; Supp. Table 3) [47]. We found four glial subtypes: astrocytes, cortex/chiasm, perineurial, and subperineurial glia (Fig. 2f; Supp. Table 3). Known glial-quiescent neuroblast signaling molecules were differentially regulated in the cortex/chiasm glia and surface glia

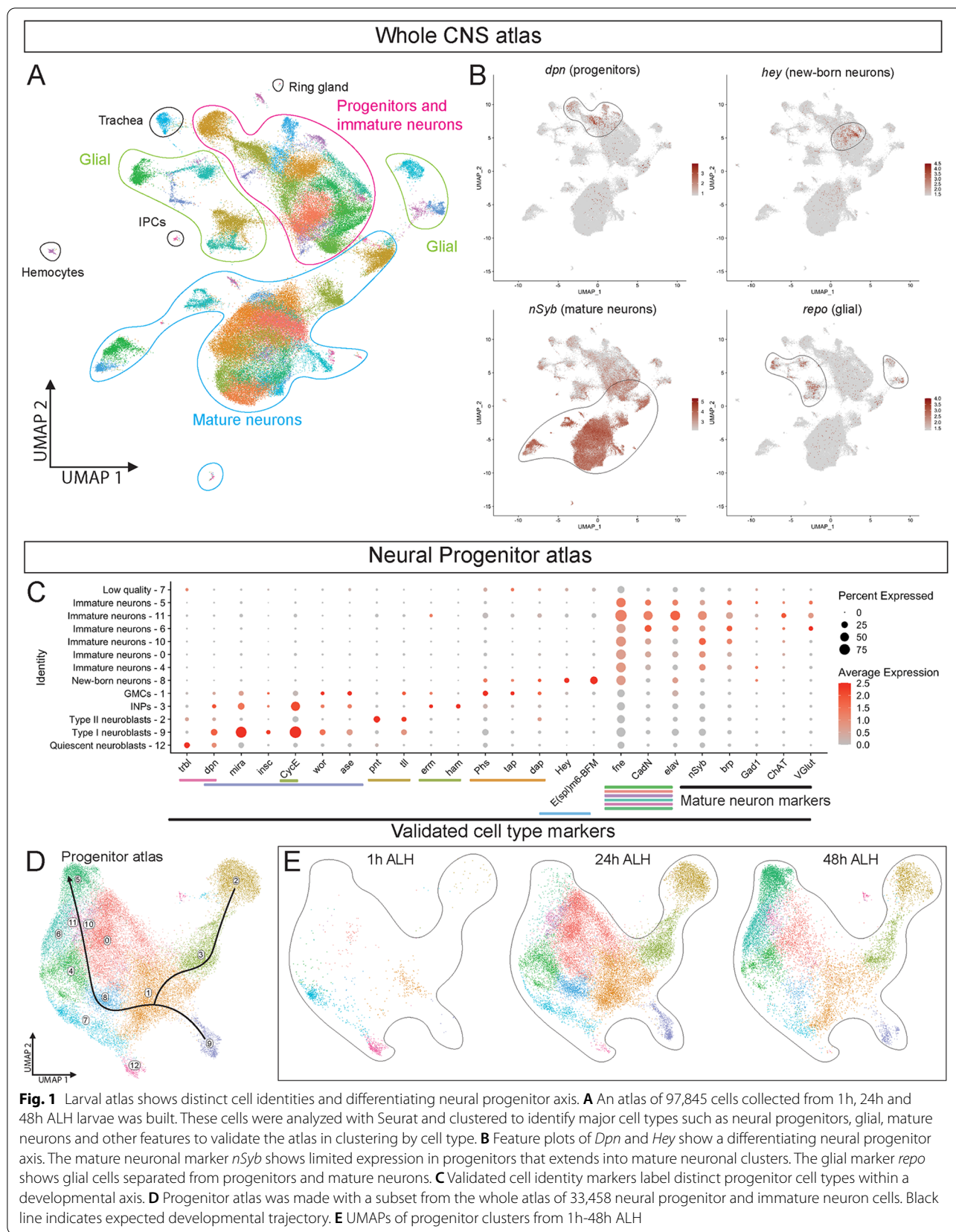


**Table 1** Validated markers for progenitors and young neurons

Cell type	Marker	References
Neuroblast, quiescent	Tribbles +	[29]
	Deadpan+	[29]
	Worniu -	[29]
Neuroblast, Type I	Deadpan +	[30]
	Asense +	[31]
	Worniu +	[32]
	Miranda +	[33]
	Inscuteable +	[34]
	String +	[34]
	Cyclin E +	[35]
Neuroblast, Type II	Pointed +	[36]
	Tailless +	[37]
	Asense -	[31]
INP	Erm +	[38]
	Hamlet +	[37]
	Cyclin E +	[25, 39]
GMC	Target of Poxn +	[25]
	Dacapo +	[40]
	Miranda -	[33]
Neuron, new-born	Hey +	[41]
	E(spl)m6BFM +	[25]
Neuron, immature	Elav+	[42]
	Ncad+	[43]
	Fne +	[44]
	Brp-	[45]
	nsyb-	[46]
Neuron, mature	Brp+	[45]
	nSyb+	[46]

**Table 2** Validated markers for glial cell types

Cell type	Marker	References
All glial	Repo +	[47, 48]
Astrocyte/neuropil glial	Gat +	[49]
	Alarm +	[50]
Perineurial	CG6126 +	[51]
	Indy +	[52]
	CG4797 +	[12]
Subperineurial	Moody +	[53]
	AdamTS-A +	[52]
Cortex/chiasm glial	Wrapper +	[54]
	Hoe1 +	[12]

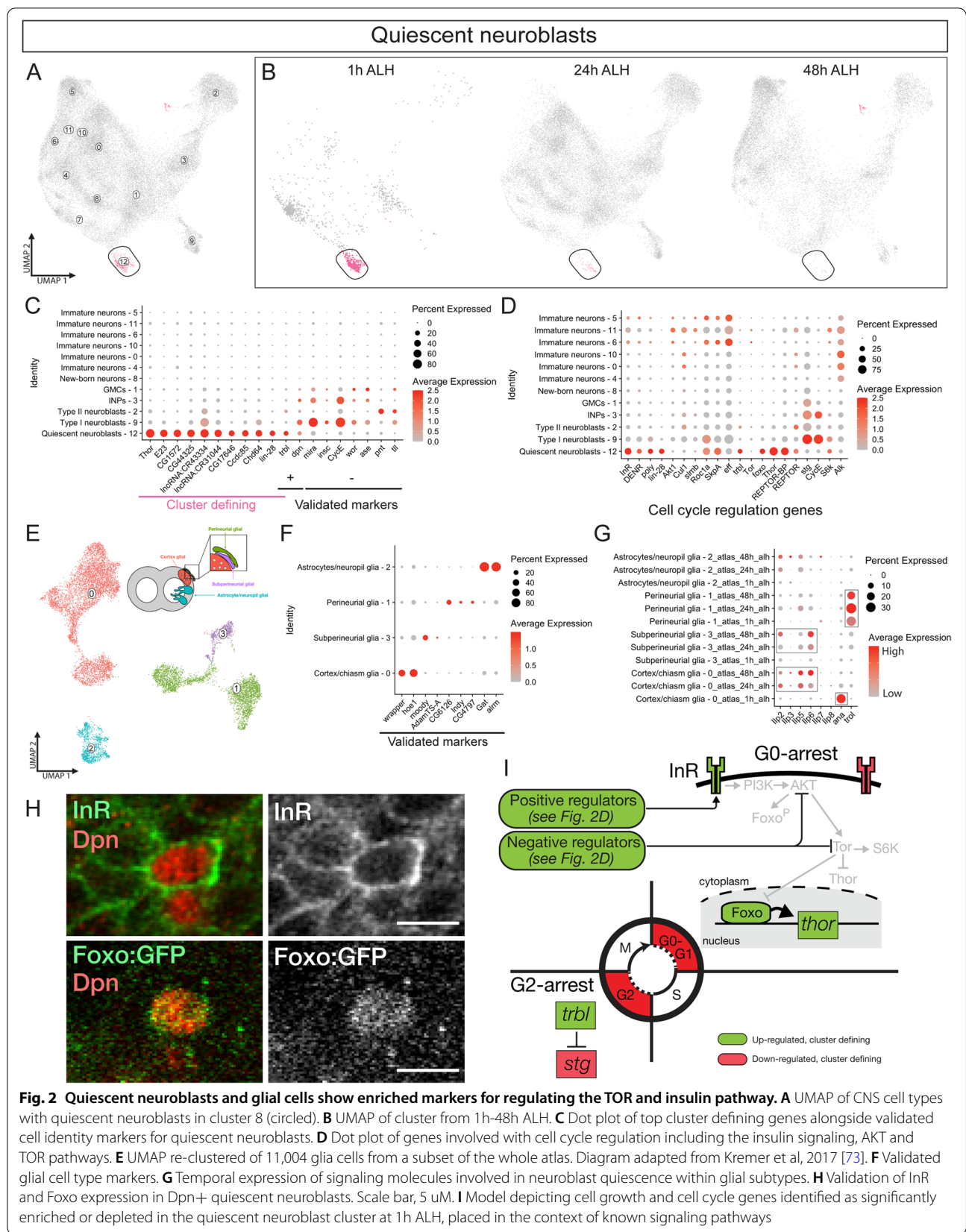
between 1h and 24h when quiescent neuroblasts are re-activated. Expression of these genes was maintained in glia along with proliferating neuroblasts at later stages of larval development (Fig. 2g; Supp. Tables 4, 5 and 6). For

**Table 3** Validated markers for mature neuron cell types

Cell type	Marker	References
Undifferentiated	Hdc+	[55]
	Ncad+	[43]
Cholinergic	Ace +	[56]
	ChAT +	
GABAergic	Gad1 +	[57]
Glutamatergic	VGlut +	[58]
Monoaminergic	Vmat +	[59]
	Ddc +	[60]
	Trh +	[61]
	Dimm +	[62]
Peptidergic	CCAP +	[62]
	Burs +	[63]
	AstC +	[64]
Octopaminergic	Vmat +	[59]
	Tbh +	[65]
	Tdc2 +	[66]
Motor neurons	Twit +	[67]
Kenyon cells $\gamma$	Rgk1	[68]
	Pka (R1/2, C1)	[69]
Neurosecretory cells	ITP	[70]
	sNPF	[70]

example, Ana, a glial secreted glycoprotein that inhibits neuroblast proliferation [75], was upregulated in cortex/chiasm glia at 1h (Fig. 2g; Supp. Table 4). Insulin-like peptides (IIPs), known to be secreted by glia and promote neuroblast exit from quiescence [28], were upregulated in cortex/chiasm glia and subperineurial glia at 24h and 48h (Fig. 2g; Supp. Tables 4 and 5). Trol, a secreted molecule acting downstream of Ana to promote neuroblast proliferation [76], was upregulated in perineurial glia at 24h (Fig. 2g; Supp. Table 6).

We validated two key regulators of quiescence, InR and Foxo, by antibody staining. Both proteins are enriched in Dpn+ quiescent neuroblasts in newly hatched larvae (Fig. 2h). We conclude that known regulators of neuroblast quiescence are expressed in cortex and surface glia at times consistent with a role in regulating the timing of neuroblast exit from quiescence. We postulate testable models for this neuroblast cell state transition (Fig. 2i). Our data supports the notion that quiescent neuroblasts express some, but not all, elements of the insulin signaling pathway (Fig. 2i), thereby transcriptionally priming them for rapid exit from quiescence. Furthermore, both cortex/chiasm and surface glia express *Ilp* genes, suggesting a shared role in signaling neuroblasts to exit quiescence. Future work will be required to further validate these models and regulatory pathways within larval quiescent neuroblasts.



### Proliferating neuroblasts shows candidate novel markers and temporal transcription factors

Here we focus on exploring gene expression in the proliferating type I and type II neuroblasts, beginning with the type I neuroblast population. We identified a type I neuroblast cluster (cluster 9; Fig. 3a,b) based on multiple validated progenitor and Type I neuroblast specific markers including: *CycE*, *str*, *wor*, *ase*, *dpn*, *mira* and *insc* plus lack of the type II specific marker *pointed* (Fig. 3c; Table 1; Supp. Table 2). The type I neuroblast cluster was most prominent at 24h and 48h (Fig. 3b), most likely due to neuroblasts at 1h being partitioned into the quiescence neuroblast cluster (see above). Not surprisingly, all markers except for *insc* were found to be cluster defining genes, demonstrating the robustness of the progenitor atlas in clustering by known cell type markers (Fig. 3c, right). The top cluster defining genes include known progenitor genes such as *Pen* (also called *oho31*), *grh* and *Syp* [39, 77–79]. In addition, we noticed novel genes in Type I neuroblasts that are uncharacterized such as several long non-coding RNAs and *CG13305* (Fig. 3c, left). These cluster defining genes are novel candidate markers for Type I neuroblasts.

Neuroblasts are known to have temporal transcription factor (TTF) cascades [80]. To identify novel candidate TTFs, we identified differentially expressed transcription factors between 24h and 48h type I neuroblasts (Fig. 3d;

Supp. Table 7). Surprisingly, we only found candidate transcription factors upregulated at 24h (24h > 48h), but not the opposite (48h > 24h). Validated TTFs for type II neuroblasts [81, 82] show their expected trend between 24h and 48h, with the exceptions of unexpected early expression of *EcR* and *Br* at 24h compared to their published expression only after 60h [81, 82]. This could be due to the presence of mRNA but not protein (i.e. post-transcriptional regulation) or due to detection of multiple isoforms with some isoforms only expressed after 60h. Our findings identify novel candidate type I neuroblast TTFs.

We identified a type II neuroblast cluster (cluster 2; Fig. 4a-b) based on the validated type II neuroblast markers *pnt* and *tll* with minimal expression of the negative marker *ase* (Fig. 4f; Supp. Table 2). As with the type I cluster, the type II cluster showed the most cells at 24h and 48h cells (Fig. 4b), consistent with the known type II neuroblast quiescent phase at 1h [28]. Further sub-division of cluster 2 showed two distinct clusters, one with substantially higher expression of type II neuroblast markers *pnt*, *tll* and *dpn* (Fig. 4e; Supp. Table 8). We identified this sub cluster as type II neuroblasts and were unable to annotate the other progenitor cluster (Fig. 4c); the unknown subcluster is not enriched for optic lobe neuroblasts nor is it enriched for low quality cells. We suspect the unannotated cluster is also

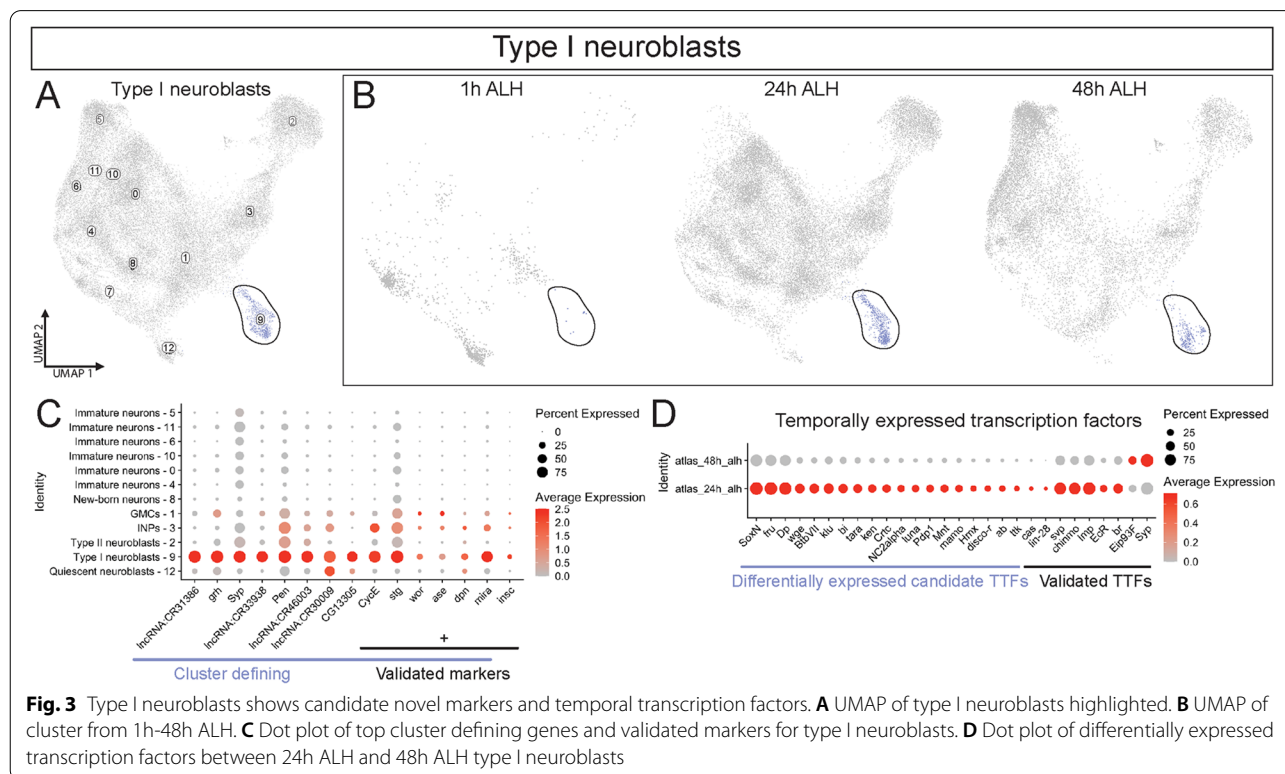
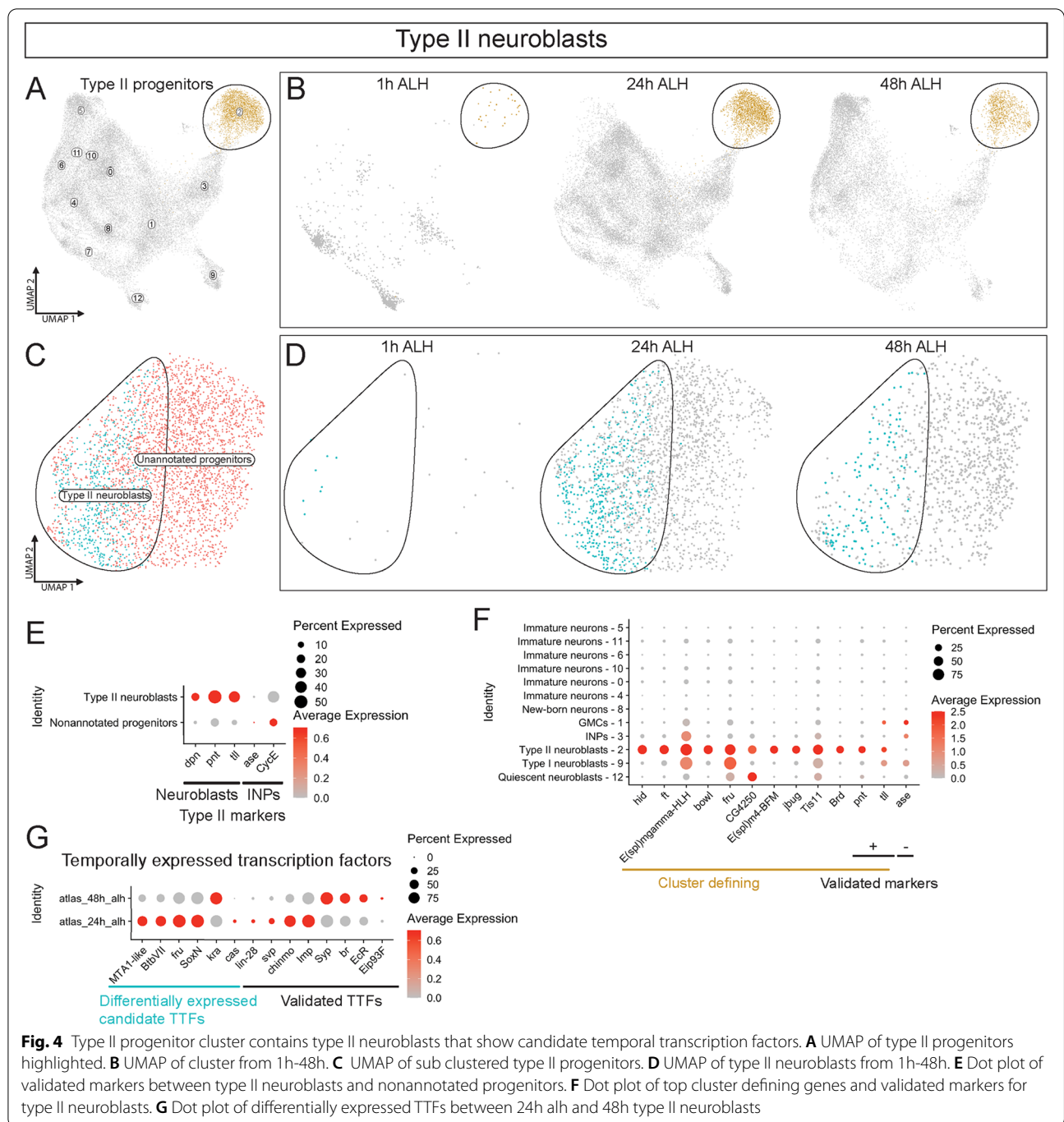


**Fig. 3** Type I neuroblasts shows candidate novel markers and temporal transcription factors. **A** UMAP of type I neuroblasts highlighted. **B** UMAP of cluster from 1h-48h ALH. **C** Dot plot of top cluster defining genes and validated markers for type I neuroblasts. **D** Dot plot of differentially expressed transcription factors between 24h ALH and 48h ALH type I neuroblasts



composed of type II progenitors given their similarity to the type II neuroblasts and slight expression of the INP markers *CycE* and *ase* expression (Fig. 4e). These type II neuroblasts had a similar trend to type I neuroblasts in being more prevalent at 24h and 48h than at 1h (Fig. 4d). Top cluster defining genes for cluster 2 included genes specific to type II neuroblasts but also expressed in type I neuroblasts and INPs (Fig. 4f).

Interestingly, the uncharacterized gene *CG4250* was exclusive to type II and quiescent neuroblasts.

We focused on identifying novel candidate TTFs between 24h and 48h in the sub-clustered type II neuroblast population. We found that validated TTFs (Fig. 4g; Supp. Table 9) followed the temporal trend previously described [80]. In addition, several novel candidate TTFs were differentially expressed between 24h and 48h

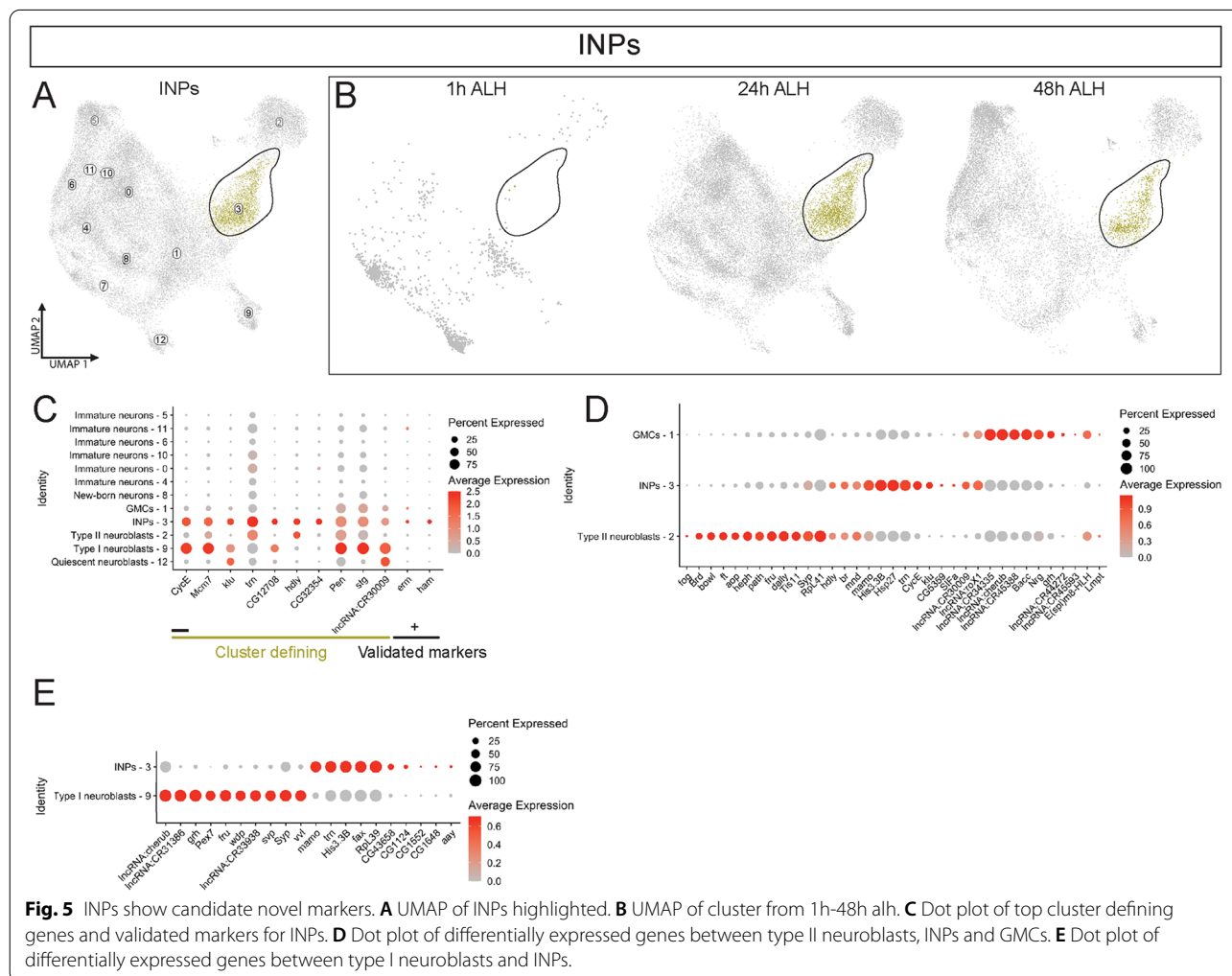
(Fig. 4g). The factors *BtbVII*, *fru* and *SoxN* show expression at 24h similar to the identified Type I neuroblast candidate TTFs. Our findings identify novel candidate type II neuroblast TTFs.

**INPs express candidate novel cell type markers**

Type II neuroblasts are unique among neuroblasts by producing INPs that generate a series of 4–6 GMCs, which each produce a pair of neurons. Type I neuroblasts in the VNC and optic lobe generate GMCs, which produce just two progeny neurons. In this way, INPs are more similar to type I neuroblasts than to GMCs. INPs can be identified by the expression of general progenitor markers (*dpn*, *ase*, *mira*, *wor*) and previously validated INP-specific gene expression of *erm* (also called *fezf2*) and *ham* (Fig. 5c; Table 1; Supp. Table 2). INPs were located near the type II neuroblasts on the UMAP plots, consistent with being derived from type II neuroblasts (Fig. 5a). As expected, we detected almost no INPs at

1h (Fig. 5b, left); these are likely to be INPs produced by embryonic type II neuroblasts [83] that are in quiescence at 1h. By 24h the type II neuroblasts have exited from quiescence and have generated a pool of INPs (Fig. 5b, center) which is maintained at 48h ALH (Fig. 5b, right). We identified a number of cluster defining genes including a proliferating INP marker *CycE* (Fig. 5c). These genes are excellent candidates for selective expression in INPs and could play a role in regulating INP-specific aspects of development and function; this hypothesis awaits validating gene expression and function.

INPs are located on the “progenitor” side of the UMAP plot, nestled between their progenitor (cluster 2, type II neuroblasts) and progeny (cluster 1, GMCs; Fig. 5a). Thus, we directly compared expression of cluster defining genes for all three cell types and found clear differences in gene expression (Fig. 5d; Supp. Tables 10 and 11). We hypothesize that these genes may play a role in distinguishing the fate of all three progenitor types.



INPs share a cell division pattern that is similar to type I neuroblasts (both producing a series of GMCs) as well as share expression of many pan-neuroblast genes (e.g. *dpn*, *mira*, *insc*, *wor*, *ase*; Fig. 1c; Table 1). Thus, we wondered how different INPs and type I neuroblasts were by scRNA-seq. We found that while many genes shared expression profiles in the two cell types, we were able to identify a number of genes that showed selective expression in INPs or type I neuroblasts (Fig. 5e; Supp. Table 12). In particular, we found several long non-coding RNAs expressed specifically in type I neuroblasts, and several previously uncharacterized genes expressed specifically in INPs. We note that *grainy head* (*grh*) is known to be expressed in both type I neuroblasts and late in some INP lineages [84–88], and it shows up as more strongly expressed in neuroblasts than INPs in our analysis (Fig. 5e). We conclude that INPs and type I neuroblasts have distinctive gene expression profiles, and that these differentially expressed genes are good candidates for distinguishing cell lineage and/or cell fate differences between these progenitors.

#### GMCs, new-born neurons and immature neurons express candidate novel cell type markers

Here we focus on the more fate-restricted GMCs, derived from type I neuroblasts and INPs, and their immature neuron progeny. GMCs were positive for the validated markers *dap* and *tap*; represented in cluster 1 (Fig. 6a,g; Table 1; Supp. Table 2). We identified new-born neurons by the Notch target *Hey*, which is expressed in new-born neurons following asymmetric division of GMCs into one Notch<sup>ON</sup> neuron (*Hey*+) and one Notch<sup>OFF</sup> neuron (*Hey*-) [41, 89]; new-born neurons are represented in cluster 8 and include both *Hey*+ Notch<sup>ON</sup> neurons and *Hey*- presumptive Notch<sup>OFF</sup> neurons (Fig. 6c,h; Table 1). We annotated immature neurons by the expression of published immature neuron markers and absence of mature neuron markers, and are represented in clusters 0, 4–6, 8, 10, and 11 (Fig. 6e,i; Table 1). Clusters 0 and 4 are the first immature neuron clusters to appear at 24h, closest to the new-born neurons and show the weakest expression of mature neuron markers (Fig. 6e–f,i). Conversely, clusters 5, 6 and 11 appear at 48h, are further from the new-born neurons and have the highest expression of neurotransmitters. We hypothesize that these distinct immature neuron clusters provide a

differential axis given their temporal, spatial and gene marker expression patterns.

Interestingly, the three cell types (GMC, new-born neuron, and immature neuron) formed a differentiation axis from right to left in the UMAP plot (Fig. 6a,c,e); as expected, each of the three cell types were under-represented at 1h when most neuroblasts are quiescent and not producing progeny (Fig. 6b,d,f). We note that progenitors are dividing throughout larval life and add complexity to the data set given each timepoint will have each of these defined transitory cell types.

In addition to the validated cell type markers, we found potential novel markers for each cell type that drove cluster assignments. Top cluster defining genes for GMCs were shared with other progenitor cell types, but several were GMC specific including *sprr* and *cas* (Fig. 6g; Supp. Table 2). New-born neuron cluster defining genes included the validated markers *Hey* and a second putative Notch target gene *E(spl)m6-BFM* (Fig. 6h; Table 1; Supp. Table 2). The six immature neurons clusters were defined by expression of known immature neuron markers and absence of known mature neuron markers such as neurotransmitter biosynthetic genes (Fig. 6i; Table 1; Supp. Table 2).

To determine candidate novel markers that distinguish cell types along the differentiation axis, we compared each cluster for their top differentially expressed genes relative to the developmentally adjacent cell type. We grouped all 6 immature neuron clusters as a single cell type for comparison. We found distinct novel candidate markers that showed markers exclusive to individual cell types and shared between them (Fig. 6j; Supp. Tables 13, 14 and 15). Interestingly, we found type I neuroblasts and immature neurons had the most specific candidate markers (Fig. 6j, left and right) while GMCs and new-born neurons contained candidate markers shared more widely (Fig. 6j, middle). We conclude that our progenitor atlas reveals a robust gene expression along a differential axis from progenitors to immature neurons with novel candidate markers and expression profiles present in each cell type.

#### Mature neurons show temporally distinct groups of transcription factors and cell surface molecules

To investigate temporal changes in mature neurons, we subclustered 51,596 cells from clusters positive

(See figure on next page.)

**Fig. 6** GMCs, new-born neurons and immature neurons show candidate novel markers. **A** UMAP of GMCs highlighted. **B** UMAP of GMCs from 1h–48h alh. **C** UMAP of new-born neurons highlighted. **D** UMAP of new-born neurons from 1h–48h alh. **E** UMAP of immature neurons highlighted. **F** UMAP of immature neurons from 1h–48h alh. **G–I** Dot plot of top cluster defining genes and validated markers for: **G** GMCs **H** New-born neurons **I** Immature neurons. **J** Differentially expressed genes between type I neuroblasts, GMCs, new-born neurons and immature neurons.





differentiated within this population of mature neurons (Fig. 7c, left). We further investigated the difference between the two clusters and found differential expression of cell surface molecules and neural differentiation genes such as *Toll-6/7*, *beat-IIa*, *jim* and *pros* (Fig. 7d; Supp. Table 17).

To identify temporally expressed genes within mature neurons, we focused on the remaining nine differentiated and annotated clusters within our mature neuron atlas. To circumvent the differences in cell number between clusters that may weight gene expression of larger clusters disproportionately, we found the top temporally expressed genes for each cluster and only included genes found in more than one cluster to reduce noise. We identified the top temporally expressed genes between all three time points (Fig. 7e; Supp. Tables 18, 19, 20, 21, 22, 23, 24, 25, 26 and 27). Notably, 24h and 48h neurons are more similar to each other than 1h neurons (Fig. 7e, middle), perhaps due to most 1h mature neurons being produced during embryogenesis, whereas the other clusters likely contain neurons produced during larval stages.

We further explored stage-specific differences by finding temporally expressed cell surface molecules and transcription factors in at least three out of the nine clusters (Fig. 7f,g; Supp. Tables 28 and 29). At 1h, there was an upregulation of several neurotransmitter receptors and neuroligins (Fig. 7f, left). At 24h, there was an upregulation of several cell adhesion molecules, while 48h showed no upregulation of cell surface molecule genes (Fig. 7f, middle). Interestingly, *Alk* and *Eph* were downregulated at 48h (Fig. 7f, right). We identified over a dozen transcription factors upregulated at 1h (Fig. 7g, left). Not surprisingly, 24h and 48h also were enriched for distinct groups of similar transcription factors (Fig. 7g, right). These temporally expressed genes provide novel candidates for molecules involved with dynamic roles such as synaptic wiring and neuronal function.

We found that our mature neuron atlas contains a diversity of neuronal types across all time points. We provided evidence that 1h mature neurons had more differentially expressed genes compared to 24h and 48h across top markers and transcription factors, suggesting mature neuron gene expression is more temporally dynamic prior to 24h. We conclude that we have identified candidate temporal markers within mature larval neurons.

## Discussion

Several scRNA-seq atlases of *Drosophila* larvae have been created [12, 15, 18, 20, 25, 90, 91]; however, few studies have offered multiple time points [21] but none to our knowledge have done so for the whole larval CNS as in our work (Fig. 1). Although other scRNA-seq analyses have provided and validated cell type markers [12,

15, 18, 20, 25, 90, 91], we provide novel candidate temporal factors within multiple cell types and lineages. It remains to be seen if the novel candidate markers we state here are validated *in vivo* and what their role is during development. Our work emphasizes the robustness of scRNA-seq data as supporting previously known gene expression profiles within specific cell types and providing strong candidate genes to explore. We provide access to our whole larval atlas and analysis as an easy to explore resource for the community (see Methods).

We note that some of our scRNA-seq samples had low sequencing depth and low read mapping (see Methods). Nevertheless, our whole atlas of 97,845 cells revealed a diversity of cell types: it identified all known progenitor cell types as well as many known mature neuronal types, including some that are quite rare (e.g. neurosecretory cells or insulin producing cells). The atlas contained three developmental time points (1h, 24h and 48h), and we still observed a robust differentiation axis within progenitors: from neuroblasts to neurons within UMAP plots. This further highlights the reliability of a scRNA-seq approach. In the future it would be beneficial to include additional time points across all developmental stages from embryo to adult.

## Quiescent neuroblasts and glial signaling

Neuroblasts enter a quiescent state in the late embryo and exit in the early larvae [28]. A challenge in studying quiescent neuroblasts has been the lack of cell specific markers, given their loss of canonical neuroblast markers [28, 92]. We found that quiescent neuroblasts formed a distinct cluster in the UMAP plots, the first time scRNA-seq methods have identified quiescent neuroblasts. Interestingly, the RNA-binding protein Lin-28, known to be expressed in neuroblasts at early larval stages [81, 82, 93, 94] was a cluster defining gene for quiescent neuroblasts. Lin-28 has been previously shown to play a role in regulating InR in intestinal stem cells [95]. This fits with our findings that quiescent neuroblasts are transcriptionally primed to respond to insulin signaling without expressing the cell cycle and cell growth genes that are activated upon exit from quiescence (Fig. 2h). It would be interesting to investigate other genes regulating the insulin signaling pathway as neuroblast early TTFs. It would also be interesting to test the function of the identified but uncharacterized neuroblast quiescence cluster defining genes.

Glia are known to maintain neuroblast quiescence as well as promote neuroblast reactivation via secreted signaling molecules [28, 75, 76]. As expected, we found both cortex and surface glia upregulate *ilps* at developmental times coinciding with exit from neuroblast quiescence

(Fig. 2i). This provides evidence supporting the model that cortex glia express *ana* during early larval development to maintain quiescent neuroblasts while perineurial surface glia upregulate *trol* to signal an exit from quiescence. Future work should test if these glia subtypes are indeed responsible for regulating neuroblast quiescence.

#### TTFs in type I and type II neuroblasts

Embryonic neuroblasts have well characterized TTF cascades [80], but it is likely that only a fraction of larval neuroblast TTFs have been identified, and even fewer have been functionally characterized. Identifying larval TTFs is complicated by larvae containing both type I and type II neuroblasts that may have similar but not identical TTFs expressed synchronously in both neuroblast populations [81, 82]. Moreover, different TTFs may be used in each type of neuroblast due to their different cell lineage (type I neuroblasts bud off GMCs while type II neuroblasts bud off INPs). Our analysis of type I and type II neuroblasts identified novel candidate TTFs with some shared and other exclusive to one of these neuroblast types. We note that identifying temporally expressed genes is difficult with only two time points, but our work should narrow the time window for validating these candidate TTFs as early expressed factors. Future work should not only explore validating these TTFs but also probing scRNA-seq data to find additional TTFs at later time points in larval development.

#### Intermediate neural progenitors

INPs are produced from type II neuroblasts and add an additional TTF cascade in their divisions prior to producing GMCs [84]. Unfortunately, we were unable to provide candidate TTFs for INPs given the challenge of distinguishing INP specific TTFs from ones carried over from the type II neuroblast TTF cascade. Our analysis indicates transcriptional similarity between INPs and Type I neuroblasts with sharing common cluster defining genes (Fig. 5c). Despite the similarity between the cell types, we found differentially expressed genes that offer promising candidate genes that could underlie the different roles of these neural progenitors. This brings up an unexplored question of whether INPs and type I neuroblasts follow the same larval TTF cascade given their similarity in lineage (both produce a series of GMCs). We hypothesize that common TTFs are likely but also expect transcriptional differences that could be tested for cell type specific functions.

#### The transition from progenitor to post-mitotic neurons

The transition from GMCs to newly born neurons marks a distinct developmental shift as a progenitor cell type becomes committed to a post-mitotic state. We noticed

that cluster defining genes for GMCs were broadly expressed in progenitors while defining genes for newborn neurons were broadly expressed in immature neurons (Fig. 5g-h). This indicates a distinct transcriptional change captured in our analysis. We note that the GMC cluster was unexpectedly defined by *cas* expression, previously known for its expression and function in neuroblasts [96–98]; our results suggest *cas* should be re-evaluated for a functional role in GMCs. Future scRNA-seq work should keep in mind that candidate genes found represent transcripts not proteins; it is likely that these are not the same patterns for many genes due to post-transcriptional regulation.

Immature neurons represent an ambiguous cell identity that is poorly described in the literature, and there are few reliable markers [99, 100]. Our analysis found candidate markers that may bridge this gap. Curiously, our immature neurons were composed of six clusters; yet we were able to define it as a single cell type with the limited validated cell makers. Our cluster defining genes closely resemble those found in Michiki et al. [25] as novel neuronal markers differentially expressed over pseudotime. Additionally, our immature neuron clusters followed a developmental projection away from progenitors in both UMAP space and temporally (Fig. 1d-e). Thus, each of the six immature neuron clusters may represent discrete differentiation states within immature neurons. Alternatively, each cluster may represent neuroblast lineage-specific, segment-specific, or region-specific (e.g. central brain vs VNC). We did not observe differential expression of Hox genes in each cluster (data not shown), ruling out anterior/posterior regional clusters. Investigating how immature neurons form six discrete clusters is an interesting question for the future.

#### Mature neurons show novel temporal changes

Mature neurons have been extensively studied to understand their unique neurotransmitter expression down to rare subtypes [101–105], yet limited efforts have explored temporal changes within the same neuronal identities across development. We found significant changes in gene expression across early larval development within mature neurons. Most notably, we found one neuron cluster specifically only present at 24h and a different neuron cluster only expressed at 48h (Fig. 7b). We suspect that these clusters represent larval neurons born at different times and thus become differentiated at different times. If our suggestion is correct, it would show that larval born neurons can differentiate asynchronously, rather than differentiation being triggered for all larval born neurons at a single timepoint.

Previous larval scRNA-seq datasets have characterized temporally expressed neurons within specific cell types

[20, 21]. In contrast, our analysis found global temporal changes shared across almost all differentiated neurons and provided interesting candidate genes for future functional assays (Fig. 7e-g). We noticed the most significant changes occurred between 1h and 24h. Surprisingly, we found many genes encoding “mature” neuron functions were upregulated at 1h. For example, various neurotransmitter receptors and the synaptic connectivity molecules *Nlg2* and *Nlg3*. This is likely due to the presence of embryonic-born differentiated neurons at 1h after larval hatching. These findings suggest that establishing neuronal connectivity is persisting from late embryos into newly hatched larvae.

## Conclusions

While much of the *Drosophila* genome has been extensively studied, there remains many uncharacterized genes. Our scRNA-seq analysis, similar to others [14, 24, 25, 81], can provide testable hypotheses for gene function based on cell type specific gene expression or co-expression with genes of a known function. We found many computational genes (CGs) with cell type-specific expression, as well as long noncoding RNAs. Both classes are likely to provide new insights into CNS development and function.

## Materials and methods

### Single cell isolation and sequencing

We analyzed a single-cell RNA-sequencing reads from dissociated cells collected from dissected *Drosophila* larval CNS tissue from 1h, 24h and 48h after larval hatching [27]. The raw sequencing data was obtained from GEO under the accession code GEO : GSE135810. In this study, we only used the following samples for analysis to enrich for larval neural progenitors: GSM4030593, GSM4030594, GSM4030597, GSM4030595, GSM4030596, GSM4030600, GSM4030601, GSM4030606, GSM4030602, GSM4030603, GSM4030604, GSM4030605, GSM4030607, GSM4030613, GSM4030614.

### scRNA-seq analysis

Our bioinformatic analysis was performed using Cell Ranger software (Version 6.0.1, 10x Genomics, Pleasanton, CA, USA) and the Seurat R package version 4.0.4 [106]. Briefly, Cell Ranger was used to perform demultiplexing, alignment, filtering, and counting of barcodes and UMIs, with the output being a cell-by-genes matrix of counts. Additionally, Cell Ranger was used to aggregate cells from multiple samples for each time point into single feature-barcode matrices. To further ensure that only high-quality cells were retained, we removed any

cells with fewer than 200 unique features and more than 20% mitochondrial RNA.

Principal component analysis was performed with cells as samples and gene expression levels as features. The top principal components (PCs) were retained as features for downstream analyses as determined by Elbow plots. We used 50 PCs for the main atlas and most of the following clusters as this provided a compromise of significant PCs and computational cost to run downstream analyses. Based on these top PCs, cells were clustered using the original Louvain algorithm approach in Seurat. Cluster resolution was determined by optimizing clusters to fit validated markers to ensure capturing an appropriate number of cell types. In order to visualize the results of the analysis, the top PCs were used to perform a non-linear embedding into two dimensions using the UMAP algorithm.

Differentially expressed genes within clusters were determined to be expressed in at least 10% more cells within the cluster(s) of interest compared to other clusters. Additionally, the average log fold change of expression cut off was 0.1 or more. We kept differentially expressed genes only if the adjusted p-value in a Wilcoxon Rank Sum test was below a threshold of 0.05. Dot plots show the average expression level of genes across all cells within the class. Temporally expressed genes were determined between time points in the atlas with similar number of cells. 1h cells were excluded from progenitor temporal analyses but kept with the mature neuron atlas given their approximately equal representation within the data sets.

### Subclustering for further Seurat analysis

A total of 33,458 cells were identified as either neural progenitors or immature neurons within the whole atlas based on their cluster defining gene expression of validated markers specified in Table 1. We reclustered these cells and kept 50 PCs as we did with the whole atlas and adjusted the cluster resolution to 0.49 as it provided biologically supported cell types as we identified all known progenitors with the fewest number of clusters. Differentially expressed genes were determined as described above. A total of 11,004 cells in *repo* positive clusters were labeled as glia and reclustered. We kept 50 PCs and adjusted the resolution to 0.045 as it provided the minimum number of clusters that strongly fitted known glia subtypes based on validated cell markers. We subclustered the progenitor atlas cluster 2, which we labeled as type II neuroblasts given *pnt* and *tll* expression. We kept 50 PCs and a resolution of 0.1 to show two clusters that were separated based on known cell type makers, e.g. a strong type II neuroblast cells and type II like progenitors were distinct. We subclustered 51,596 cells from *Brp*

and *nSyb* positive clusters. Again, we kept 50 PCs but changed the cluster resolution to 0.37 as it provided the minimum number of clusters while capturing all known neuronal cell types that we could identify in the data.

#### Data and code availability

All code used for analyses with the corresponding Cell Ranger outputs and Seurat objects are available at ([https://www.dropbox.com/sh/iilbqlqysgyocbu/AAADar0UdyA1Ep5qsHtRhiq\\_da?dl=0](https://www.dropbox.com/sh/iilbqlqysgyocbu/AAADar0UdyA1Ep5qsHtRhiq_da?dl=0)). scRNA-seq data is accessible under the accession code GEO: GSE135810.

#### Protein localization

Standard methods were used for immunofluorescent staining [107]. The line for the foxo:GFP fusion protein is *MI00493-GFSTF0* (BDSC#59,766) detected with anti-GFP immunofluorescence. Primary antibodies and sources: chicken anti-GFP (1:500; Abcam 13,970, Cambridge, MA, USA), rat anti-Dpn (1:100; Abcam), guinea pig anti-InR (1:500; Siegrist lab). Secondary antibodies were from Jackson ImmunoResearch and used according to product recommendation. Images were collected on a Leica SP8 laser scanning confocal microscope (Leica, Wetzlar, Germany) equipped with a 63×, 1.4 NA oil-immersion objective.

#### Supplementary Information

The online version contains supplementary material available at <https://doi.org/10.1186/s13064-022-00163-7>.

Additional file 1.  
Additional file 2.  
Additional file 3.  
Additional file 4.  
Additional file 5.  
Additional file 6.  
Additional file 7.  
Additional file 8.  
Additional file 9.  
Additional file 10.  
Additional file 11.  
Additional file 12.  
Additional file 13.  
Additional file 14.  
Additional file 15.  
Additional file 16.  
Additional file 17.  
Additional file 18.  
Additional file 19.  
Additional file 20.  
Additional file 21.

Additional file 22.  
Additional file 23.  
Additional file 24.  
Additional file 25.  
Additional file 26.  
Additional file 27.  
Additional file 28.  
Additional file 29.

#### Acknowledgements

We thank Sen-Lin Lai, Cheng-Yu Lee, and Sarah Ackerman for comments on the manuscript. Funding was provided by an NIH Training Grant 5-T32-HD07348 (ND), NIH HD27056 (ND), and HHMI (CQD).

#### Additional information

Funder: Howard Hughes Medical Institute, no referee number; NIH R01 HD27056 (Chris Doe). NIH R35 GM141886 (Sarah Siegrist). The funders had no role in study design, data collection and interpretation, or the decision to submit the work for publication.

#### Authors' contributions

ND performed RNA-seq analysis, generated all figures, and wrote the manuscript. BC, LLM, ABK and MZ generated the RNA-seq data; CS, XY, and SES generated Fig. 2 H and provided comments on the manuscript. CQD supervised the project and edited figures and text. The author(s) read and approved the final manuscript.

#### Availability of data and materials

All data and materials will be placed in a public repository (e.g. github or Bloomington stock center) upon acceptance for publication.

#### Declarations

**Ethics approval and consent to participate**  
n/a.

#### Consent for publication

All authors consent for this to be published.

#### Competing Interests

None.

#### Author details

<sup>1</sup>Institute of Neuroscience, Howard Hughes Medical Institute, University of Oregon, OR 97403 Eugene, USA. <sup>2</sup>Department of Zoology, University of Cambridge, Cambridge, UK. <sup>3</sup>Department of Biology, University of Virginia, VA 22904 Charlottesville, USA. <sup>4</sup>Whitney Laboratory for Marine Biosciences, University of Florida, FL 32080 St. Augustine, USA. <sup>5</sup>MRC Laboratory of Molecular Biology, Dept of Zoology, University of Cambridge, Cambridge, UK. <sup>6</sup>Janelia Research Campus, VA, Ashburn, USA.

Received: 1 March 2022 Accepted: 19 May 2022

Published online: 24 August 2022

#### References

1. Luo L. Principles of Neurobiology. 2nd ed. Boca Raton: Garland Science; 2020.
2. Skeath JB, Thor S. Genetic control of Drosophila nerve cord development. *Curr Opin Neurobiol.* 2003;13:8–15.
3. Hobert O, Westphal H. Functions of LIM-homeobox genes. *Trends Genet TIG.* 2000;16:75–83.
4. Clark BS, Stein-O'Brien GL, Shiau F, Cannon GH, Davis-Marcisak E, Sherman T, et al. Single-Cell RNA-Seq Analysis of Retinal Development

- Identifies NFI Factors as Regulating Mitotic Exit and Late-Born Cell Specification. *Neuron*. 2019;102:1111–1126.e5.
5. Johnson MB, Walsh CA. Cerebral cortical neuron diversity and development at single-cell resolution. *Curr Opin Neurobiol*. 2017;42:9–16.
  6. Li Z, Tyler WA, Haydar TF. Lessons from single cell sequencing in CNS cell specification and function. *Curr Opin Genet Dev*. 2020;65:138–43.
  7. Chang E, Ruan X, Zhu R, Wang Y, Zhang J. Values of Single-Cell RNA Sequencing in Development of Cerebral Cortex. *Adv Exp Med Biol*. 2020;1255:231–47.
  8. Ying P, Huang C, Wang Y, Guo X, Cao Y, Zhang Y, et al. Single-Cell RNA Sequencing of Retina: New Looks for Gene Marker and Old Diseases. *Front Mol Biosci*. 2021;8:699906.
  9. Meistermann D, Bruneau A, Loubersac S, Reignier A, Firmin J, François-Campion V, et al. Integrated pseudotime analysis of human pre-implantation embryo single-cell transcriptomes reveals the dynamics of lineage specification. *Cell Stem Cell*. 2021;S1934-5909(21)00185–5.
  10. Zheng S, Papalexi E, Butler A, Stephenson W, Satija R. Molecular transitions in early progenitors during human cord blood hematopoiesis. *Mol Syst Biol*. 2018;14:e8041.
  11. Zhou W, Yui MA, Williams BA, Yun J, Wold BJ, Cai L, et al. Single-Cell Analysis Reveals Regulatory Gene Expression Dynamics Leading to Lineage Commitment in Early T Cell Development. *Cell Syst*. 2019;9:321–337.e9.
  12. Konstantinides N, Kapuralin K, Fadil C, Barboza L, Satija R, Desplan C. Phenotypic Convergence: Distinct Transcription Factors Regulate Common Terminal Features. *Cell*. 2018;174:622–635.e13.
  13. Bates AS, Janssens J, Jefferis GS, Aerts S. Neuronal cell types in the fly: single-cell anatomy meets single-cell genomics. *Curr Opin Neurobiol*. 2019;56:125–34.
  14. Croset V, Treiber CD, Waddell S. Cellular diversity in the *Drosophila* midbrain revealed by single-cell transcriptomics. *eLife*. 2018;7:e34550.
  15. Davie K, Janssens J, Koldere D, De Waegeneer M, Pech U, Kreft L, et al. A Single-Cell Transcriptome Atlas of the Aging *Drosophila* Brain. *Cell*. 2018;174:982–998.e20.
  16. Özel MN, Gibbs CS, Holguera I, Soliman M, Bonneau R, Desplan C. Coordinated control of neuronal differentiation and wiring by a sustained code of transcription factors [Internet]. *bioRxiv*; 2022 [cited 2022 May 2]. p. 2022.05.01.490216. Available from: <https://www.biorxiv.org/content/https://doi.org/10.1101/2022.05.01.490216v1>
  17. Özel MN, Simon F, Jafari S, Holguera I, Chen Y-C, Benhra N, et al. Neuronal diversity and convergence in a visual system developmental atlas. *Nature*. 2021;589:88–95.
  18. Li H, Horns F, Wu B, Xie Q, Li J, Li T, et al. Classifying *Drosophila* Olfactory Projection Neuron Subtypes by Single-Cell RNA Sequencing. *Cell*. 2017;171:1206–1220.e22.
  19. Li H, Li T, Horns F, Li J, Xie Q, Xu C, et al. Single-Cell Transcriptomes Reveal Diverse Regulatory Strategies for Olfactory Receptor Expression and Axon Targeting. *Curr Biol CB*. 2020;30:1189–1198.e5.
  20. McLaughlin CN, Brbić M, Xie Q, Li T, Horns F, Kolluru SS, et al. Single-cell transcriptomes of developing and adult olfactory receptor neurons in *Drosophila*. *eLife*. 2021;10:e63856.
  21. Xie Q, Brbić M, Horns F, Kolluru SS, Jones RC, Li J, et al. Temporal evolution of single-cell transcriptomes of *Drosophila* olfactory projection neurons. *eLife*. 2021;10:e63450.
  22. Kurmangaliyev YZ, Yoo J, Valdes-Aleman J, Sanfilippo P, Zipursky SL. Transcriptional Programs of Circuit Assembly in the *Drosophila* Visual System. *Neuron*. 2020;108:1045–1057.e6.
  23. Brunet Avalos C, Sprecher SG. Single-Cell Transcriptomic Reveals Dual and Multi-Transmitter Use in Neurons Across Metazoans. *Front Mol Neurosci*. 2021;14:623148.
  24. Marques GS, Teles-Reis J, Konstantinides N, Brito PH, Homem CCF. Fate transitions in *Drosophila* neural lineages: a single cell road map to mature neurons [Internet]. 2021 Jun p. 2021.06.22.449317. Available from: <https://www.biorxiv.org/content/https://doi.org/10.1101/2021.06.22.449317v1>
  25. Michki NS, Li Y, Sanjasaz K, Zhao Y, Shen FY, Walker LA, et al. The molecular landscape of neural differentiation in the developing *Drosophila* brain revealed by targeted scRNA-seq and multi-informatic analysis. *Cell Rep*. 2021;35:109039.
  26. Karaiskos N, Wahle P, Alles J, Boltengagen A, Ayoub S, Kipar C, et al. The *Drosophila* embryo at single-cell transcriptome resolution. *Science*. 2017;358:194–9.
  27. Corrales M, Cocanougher BT, Kohn AB, Long XS, Lemire A, Cardona A, et al. A single-cell transcriptomic atlas of complete insect nervous systems across multiple life stages. *Neural Dev*. In press.
  28. Chell JM, Brand AH. Nutrition-responsive glia control exit of neural stem cells from quiescence. *Cell*. 2010;143:1161–73.
  29. Otsuki L, Brand AH. Cell cycle heterogeneity directs the timing of neural stem cell activation from quiescence. *Science*. 2018;360:99–102.
  30. Bier E, Vaessin H, Younger-Shepherd S, Jan LY, Jan YN. *deadpan*, an essential pan-neural gene in *Drosophila*, encodes a helix-loop-helix protein similar to the hairy gene product. *Genes Dev*. 1992;6:2137–51.
  31. Bowman SK, Rolland V, Betschinger J, Kinsey KA, Emery G, Knoblich JA. The tumor suppressors *Brat* and *Numb* regulate transit-amplifying neuroblast lineages in *Drosophila*. *Dev Cell*. 2008;14:535–46.
  32. Ashraf SI, Ganguly A, Roote J, Ip YT. *Worniu*, a Snail family zinc-finger protein, is required for brain development in *Drosophila*. *Dev Dyn*. 2004;231:379–86.
  33. Ikeshima-Kataoka H, Skeath JB, Nabeshima Y, Doe CQ, Matsuzaki F. *Miranda* directs *Prospero* to a daughter cell during *Drosophila* asymmetric divisions. *Nature*. 1997;390:625–9.
  34. Ashraf SI, Ip YT. The Snail protein family regulates neuroblast expression of *inscuteable* and *string*, genes involved in asymmetry and cell division in *Drosophila*. *Development*. 2001;128:4757–67.
  35. Caldwell MC, Datta S. Expression of cyclin E or DP/E2F rescues the G1 arrest of *trf* mutant neuroblasts in the *Drosophila* larval central nervous system. *Mech Dev*. 1998;79:121–30.
  36. Zhu S, Barshow S, Wildonger J, Jan LY, Jan YN. *Ets* transcription factor *Pointed* promotes the generation of intermediate neural progenitors in *Drosophila* larval brains. *Proc Natl Acad Sci U A*. 2011;108:20615–20.
  37. Rives-Quinto N, Komori H, Ostgaard CM, Janssens DH, Kondo S, Dai Q, et al. Sequential activation of transcriptional repressors promotes progenitor commitment by silencing stem cell identity genes. Desplan C, Banerjee U, editors. *eLife*. eLife Sciences Publications, Ltd; 2020;9:e56187.
  38. Li X, Xie Y, Zhu S. Notch maintains *Drosophila* type II neuroblasts by suppressing expression of the *Fez* transcription factor *Earmuff*. *Dev Camb Engl*. 2016;143:2511–21.
  39. Yang C-P, Samuels TJ, Huang Y, Yang L, Ish-Horowitz D, Davis I, et al. *Imp* and *Syp* RNA-binding proteins govern decommissioning of *Drosophila* neural stem cells. *Dev Camb Engl*. 2017;144:3454–64.
  40. Lane ME, Sauer K, Wallace K, Jan YN, Lehner CF, Vaessin H. *Dacapo*, a cyclin-dependent kinase inhibitor, stops cell proliferation during *Drosophila* development. *Cell*. 1996;87:1225–35.
  41. Monastirioti M, Giagtzoglou N, Koumbanakis KA, Zacharioudaki E, Deligiannaki M, Wech I, et al. *Drosophila Hey* is a target of Notch in asymmetric divisions during embryonic and larval neurogenesis. *Development*. 2010;137:191–201.
  42. Robinow S, White K. Characterization and spatial distribution of the *ELAV* protein during *Drosophila melanogaster* development. *J Neurobiol*. 1991;22:443–61.
  43. Young JM, Armstrong JD. Building the central complex in *Drosophila*: the generation and development of distinct neural subsets. *J Comp Neurol*. 2010;518:1525–41.
  44. Samson M-L, Chalvet F. *found in neurons*, a third member of the *Drosophila elav* gene family, encodes a neuronal protein and interacts with *elav*. *Mech Dev*. 2003;120:373–83.
  45. Wagh DA, Rasse TM, Asan E, Hofbauer A, Schwenkert I, Dürrbeck H, et al. *Bruchpilot*, a Protein with Homology to *ELKS/CAST*, Is Required for Structural Integrity and Function of Synaptic Active Zones in *Drosophila*. *Neuron*. 2006;49:833–44.
  46. Deitcher DL, Ueda A, Stewart BA, Burgess RW, Kidokoro Y, Schwarz TL. Distinct requirements for evoked and spontaneous release of neurotransmitter are revealed by mutations in the *Drosophila* gene *neuronal-synaptobrevin*. *J Neurosci Off J Soc Neurosci*. 1998;18:2028–39.
  47. Xiong WC, Okano H, Patel NH, Blendy JA, Montell C. *repo* encodes a glial-specific homeo domain protein required in the *Drosophila* nervous system. *Genes Dev*. 1994;8:981–94.
  48. Campbell G, Goring H, Lin T, Spana E, Andersson S, Doe CQ, et al. *RK2*, a glial-specific homeodomain protein required for embryonic nerve cord condensation and viability in *Drosophila*. *Development*. 1994;120:2957–66.

49. Stork T, Sheehan A, Tasdemir-Yilmaz OE, Freeman MR. Neuron-glia interactions through the Heartless FGF receptor signaling pathway mediate morphogenesis of *Drosophila* astrocytes. *Neuron*. 2014;83:388–403.
50. Doherty J, Logan MA, Tasdemir OE, Freeman MR. Ensheathing glia function as phagocytes in the adult *Drosophila* brain. *J Neurosci*. 2009;29:4768–81.
51. FlyBase Reference Report: Fisher et al., 2012, BDGP insitu homepage. [cited 2022 Apr 30]. Available from: <http://beta.flybase.org/reports/FBrf0219073.html>
52. DeSalvo MK, Hindle SJ, Rusan ZM, Orng S, Eddison M, Halliwill K, et al. The *Drosophila* surface glia transcriptome: evolutionary conserved blood-brain barrier processes. *Front Neurosci*. 2014;8:346.
53. Bainton RJ, Tsai LT-Y, Schwabe T, DeSalvo M, Gaul U, Heberlein U. moody encodes two GPCRs that regulate cocaine behaviors and blood-brain barrier permeability in *Drosophila*. *Cell*. 2005;123:145–56.
54. Noordermeer JN, Kopczynski CC, Fetter RD, Bland KS, Chen WY, Goodman CS. Wrapper, a novel member of the Ig superfamily, is expressed by midline glia and is required for them to ensheath commissural axons in *Drosophila*. *Neuron*. 1998;21:991–1001.
55. Avet-Rochex A, Carvajal N, Christoforou CP, Yeung K, Maierbrugger KT, Hobbs C, et al. Unkempt is negatively regulated by mTOR and uncouples neuronal differentiation from growth control. *PLoS Genet*. 2014;10:e1004624.
56. Baqri R, Charan R, Schimmelpfeng K, Chavan S, Ray K. Kinesin-2 differentially regulates the anterograde axonal transports of acetylcholinesterase and choline acetyltransferase in *Drosophila*. *J Neurobiol*. 2006;66:378–92.
57. Nässel DR, Enell LE, Santos JG, Wegener C, Johard HAD. A large population of diverse neurons in the *Drosophila* central nervous system expresses short neuropeptide F, suggesting multiple distributed peptide functions. *BMC Neurosci*. 2008;9:90.
58. Daniels RW, Gelfand MV, Collins CA, DiAntonio A. Visualizing glutamatergic cell bodies and synapses in *Drosophila* larval and adult CNS. *J Comp Neurol*. 2008;508:131–52.
59. Greer CL, Grygoruk A, Patton DE, Ley B, Romero-Calderon R, Chang H-Y, et al. A splice variant of the *Drosophila* vesicular monoamine transporter contains a conserved trafficking domain and functions in the storage of dopamine, serotonin, and octopamine. *J Neurobiol*. 2005;64:239–58.
60. Beall CJ, Hirsh J. Regulation of the *Drosophila* dopa decarboxylase gene in neuronal and glial cells. *Genes Dev*. 1987;1:510–20.
61. Neckameyer WS, Coleman CM, Eadie S, Goodwin SF. Compartmentalization of neuronal and peripheral serotonin synthesis in *Drosophila melanogaster*. *Genes Brain Behav*. 2007;6:756–69.
62. Hewes RS, Park D, Gauthier SA, Schaefer AM, Taghert PH. The bHLH protein Dimmed controls neuroendocrine cell differentiation in *Drosophila*. *Dev Camb Engl*. 2003;130:1771–81.
63. Lee GG, Kikuno K, Nair S, Park JH. Mechanisms of postecdysis-associated programmed cell death of peptidergic neurons in *Drosophila melanogaster*. *J Comp Neurol*. 2013;521:3972–91.
64. Díaz MM, Schlichting M, Abruzzi KC, Long X, Rosbash M. Allatostatin-C/AstC-R2 Is a Novel Pathway to Modulate the Circadian Activity Pattern in *Drosophila*. *Curr Biol CB*. 2019;29:13–22.e3.
65. Koon AC, Ashley J, Barria R, DasGupta S, Brain R, Waddell S, et al. Autoregulatory and paracrine control of synaptic and behavioral plasticity by octopaminergic signaling. *Nat Neurosci*. 2011;14:190–9.
66. Cole SH, Carney GE, McClung CA, Willard SS, Taylor BJ, Hirsh J. Two functional but noncomplementing *Drosophila* tyrosine decarboxylase genes: distinct roles for neural tyramine and octopamine in female fertility. *J Biol Chem*. 2005;280:14948–55.
67. Kim NC, Marqués G. The Ly6 neurotoxin-like molecule target of wit regulates spontaneous neurotransmitter release at the developing neuromuscular junction in *Drosophila*. *Dev Neurobiol*. 2012;72:1541–58.
68. Murakami S, Minami-Ohtsubo M, Nakato R, Shirahige K, Tabata T. Two Components of Aversive Memory in *Drosophila*, Anesthesia-Sensitive and Anesthesia-Resistant Memory, Require Distinct Domains Within the Rgl1 Small GTPase. *J Neurosci Off J Soc Neurosci*. 2017;37:5496–510.
69. Crittenden JR, Skoulakis EM, Han KA, Kalderon D, Davis RL. Tripartite mushroom body architecture revealed by antigenic markers. *Learn Mem Cold Spring Harb N*. 1998;5:38–51.
70. Kahsai L, Kapan N, Dirksen H, Winther AME, Nässel DR. Metabolic stress responses in *Drosophila* are modulated by brain neurosecretory cells that produce multiple neuropeptides. *PLoS One*. 2010;5:e11480.
71. Truman JW, Bate M. Spatial and temporal patterns of neurogenesis in the central nervous system of *Drosophila melanogaster*. *Dev Biol*. 1988;125:145–57.
72. Prokop A, Technau GM. The origin of postembryonic neuroblasts in the ventral nerve cord of *Drosophila melanogaster*. *Dev Camb Engl*. 1991;111:79–88.
73. Kremer MC, Jung C, Batelli S, Rubin GM, Gaul U. The glia of the adult *Drosophila* nervous system. *Glia*. 2017;65:606–38.
74. Sousa-Nunes R, Yee LL, Gould AP. Fat cells reactivate quiescent neuroblasts via TOR and glial insulin relays in *Drosophila*. *Nature*. 2011;471:508–12.
75. Ebens AJ, Garren H, Cheyette BN, Zipursky SL. The *Drosophila* anachronism locus: a glycoprotein secreted by glia inhibits neuroblast proliferation. *Cell*. 1993;74:15–27.
76. Datta S. Control of proliferation activation in quiescent neuroblasts of the *Drosophila* central nervous system. *Development*. 1995;121:1173–82.
77. Küssel P, Frasch M. Pendulin, a *Drosophila* protein with cell cycle-dependent nuclear localization, is required for normal cell proliferation. *J Cell Biol*. 1995;129:1491–507.
78. Török I, Strand D, Schmitt R, Tick G, Török T, Kiss I, et al. The overgrown hematopoietic organs-31 tumor suppressor gene of *Drosophila* encodes an Importin-like protein accumulating in the nucleus at the onset of mitosis. *J Cell Biol*. 1995;129:1473–89.
79. Uv AE, Harrison EJ, Bray SJ. Tissue-specific splicing and functions of the *Drosophila* transcription factor Grainyhead. *Mol Cell Biol*. 1997;17:6727–35.
80. Doe CQ. Temporal Patterning in the *Drosophila* CNS. *Annu Rev Cell Dev Biol*. 2017;33:in press.
81. Ren Q, Yan C-P, Liu Z, Sugino K, Mok K, He Y, et al. Stem cell intrinsic, Seven-up-triggered temporal factor gradients diversify intermediate neural progenitors. *Curr Biol*. 2017;in press.
82. Syed MH, Mark B, Doe CQ. Steroid hormone induction of temporal gene expression in *Drosophila* brain neuroblasts generates neuronal and glial diversity. *Elife*. 2017;6. Available from: <https://www.ncbi.nlm.nih.gov/pubmed/28394252>
83. Walsh KT, Doe CQ. *Drosophila* embryonic type II neuroblasts: origin, temporal patterning, and contribution to the adult central complex. *Dev Camb Engl*. 2017;144:4552–62.
84. Bayraktar OA, Doe CQ. Combinatorial temporal patterning in progenitors expands neural diversity. *Nature*. 2013;498:445–55.
85. Abdusselamoglu MD, Eroglu E, Burkard TR, Knoblich JA. The transcription factor odd-paired regulates temporal identity in transit-amplifying neural progenitors via an incoherent feed-forward loop. *VijayRaghavan K, Wang H, Sen S, editors. eLife*. 2019;8:e46566.
86. Almeida MS, Bray SJ. Regulation of post-embryonic neuroblasts by *Drosophila* Grainyhead. *Mech Dev*. 2005;122:1282–93.
87. Sullivan LF, Warren TL, Doe CQ. Temporal identity establishes columnar neuron morphology, connectivity, and function in a *Drosophila* navigation circuit. *eLife*. 2019;8.
88. Farnsworth DR, Bayraktar OA, Doe CQ. Aging Neural Progenitors Lose Competence to Respond to Mitogenic Notch Signaling. *Curr Biol*. 2015;25:3058–68.
89. Mark B, Lai S-L, Zarin AA, Manning L, Pollington HQ, Litwin-Kumar A, et al. A developmental framework linking neurogenesis and circuit formation in the *Drosophila* CNS. *eLife*. 2021;10.
90. Tan L, Zhang KX, Pecot MY, Nagarkar-Jaiswal S, Lee PT, Takemura SY, et al. Ig Superfamily Ligand and Receptor Pairs Expressed in Synaptic Partners in *Drosophila*. *Cell*. 2015;163:1756–69.
91. Nguyen TH, Vicidomini R, Choudhury SD, Coon SL, Iben J, Brody T, et al. Single-Cell RNA Sequencing Analysis of the *Drosophila* Larval Ventral Cord. *Curr Protoc*. 2021;1:e38.
92. Lai SL, Doe CQ. Transient nuclear Prospero induces neural progenitor quiescence. *Elife*. 2014;3.

93. Narbonne-Reveau K, Lanet E, Dillard C, Foppolo S, Chen CH, Parrinello H, et al. Neural stem cell-encoded temporal patterning delineates an early window of malignant susceptibility in *Drosophila*. *Elife*. 2016;5. Available from: <http://www.ncbi.nlm.nih.gov/pubmed/27296804>
94. Liu Z, Yang CP, Sugino K, Fu CC, Liu LY, Yao X, et al. Opposing intrinsic temporal gradients guide neural stem cell production of varied neuronal fates. *Science*. 2015;350:317–20.
95. Chen C-H, Luhur A, Sokol N. Lin-28 promotes symmetric stem cell division and drives adaptive growth in the adult *Drosophila* intestine. *Dev Camb Engl*. 2015;142:3478–87.
96. Cui X, Doe CQ. *ming* is expressed in neuroblast sublineages and regulates gene expression in the *Drosophila* central nervous system. *Development*. 1992;116:943–52.
97. Kambadur R, Koizumi K, Stivers C, Nagle J, Poole SJ, Odenwald WF. Regulation of POU genes by *castor* and *hunchback* establishes layered compartments in the *Drosophila* CNS. *Genes Dev*. 1998;12:246–60.
98. Mellerick DM, Kassis JA, Zhang SD, Odenwald WF. *castor* encodes a novel zinc finger protein required for the development of a subset of CNS neurons in *Drosophila*. *Neuron*. 1992;9:789–803.
99. Dumstrei K, Wang F, Hartenstein V. Role of DE-cadherin in neuroblast proliferation, neural morphogenesis, and axon tract formation in *Drosophila* larval brain development. *J Neurosci Off J Soc Neurosci*. 2003;23:3325–35.
100. Young JM, Armstrong JD. Structure of the adult central complex in *Drosophila*: organization of distinct neuronal subsets. *J Comp Neurol*. 2010;518:1500–24.
101. Hobert O, Kratsios P. Neuronal identity control by terminal selectors in worms, flies, and chordates. *Curr Opin Neurobiol*. 2019;56:97–105.
102. Lodato S, Arlotta P. Generating neuronal diversity in the mammalian cerebral cortex. *Annu Rev Cell Dev Biol*. 2015;31:699–720.
103. Yasugi T, Nishimura T. Temporal regulation of the generation of neuronal diversity in *Drosophila*. *Dev Growth Differ*. 2016;58:73–87.
104. Williams EA, Jékely G. Neuronal cell types in the annelid *Platynereis dumerilii*. *Curr Opin Neurobiol*. 2019;56:106–16.
105. Farnsworth DR, Saunders LM, Miller AC. A single-cell transcriptome atlas for zebrafish development. *Dev Biol*. 2020;459:100–8.
106. Hao Y, Hao S, Andersen-Nissen E, Mauck WM, Zheng S, Butler A, et al. Integrated analysis of multimodal single-cell data. *Cell*. 2021;184:3573–3587.e29.
107. Yuan X, Sipe CW, Suzawa M, Bland ML, Siegrist SE. *Dilp-2*-mediated PI3-kinase activation coordinates reactivation of quiescent neuroblasts with growth of their glial stem cell niche. *PLoS Biol*. 2020;18:e3000721.

## Publisher's Note

Springer Nature remains neutral with regard to jurisdictional claims in published maps and institutional affiliations.

Ready to submit your research? Choose BMC and benefit from:

- fast, convenient online submission
- thorough peer review by experienced researchers in your field
- rapid publication on acceptance
- support for research data, including large and complex data types
- gold Open Access which fosters wider collaboration and increased citations
- maximum visibility for your research: over 100M website views per year

At BMC, research is always in progress.

Learn more [biomedcentral.com/submissions](https://biomedcentral.com/submissions)

